Title page

Dissociable neural substrates of integration and segregation in exogenous attention

Yu-Jie Chen[1†], Ai-Su Li[1†], Yang Yu[2], Su Hu[2], Xun He[3*] and Yang Zhang[1*]

[1] Department of Psychology, Soochow University, Jiangsu, China, 215000

[2] Department of Radiology, The First Affiliated Hospital of Soochow University, Suzhou, Jiangsu, China, 215000

[3] School of Psychology, Bournemouth University, United Kingdom

*Correspondence concerning this article should be addressed to:

Yang Zhang (Department of Psychology, Soochow University, Suzhou, China. Email: yzhangpsy@suda.edu.cn) or Xun He (School of Psychology, Bournemouth University, Poole, United Kingdom. Email: xhe@bournemouth.ac.uk)

† These authors contributed equally to the work as co-first authors

Impact Statement: This study offers the first direct neuroimaging evidence for the integration–segregation theory of exogenous attention by identifying dissociable neural signatures of the competing integration and segregation processes, strengthening the understanding of attentional orienting mechanisms.

Abstract

The integration-segregation theory proposes that early facilitation and later inhibition (i.e., inhibition of return, IOR) in exogenous attention arise from the competition between cue-target event integration and segregation. Although widely supported behaviorally, the theory lacked direct neural evidence. Here, we used event-related fMRI with an optimized cue-target paradigm to test this account. Cued targets elicited stronger activation in the frontoparietal attention networks, including the bilateral frontal eye field (FEF) and intraparietal sulcus (IPS), right temporoparietal junction (TPJ), and left dorsal anterior cingulate cortex (dACC), consistent with the notion of attentional demand of reactivating the cue-initiated representations for integration. In contrast, uncued targets engaged the medial temporal cortex, particularly the bilateral parahippocampal gyrus (PHG) and superior temporal gyrus (STG), reflecting the segregation processes associated with new object-file creation and novelty encoding. These dissociable activations provide the first direct neuroimaging evidence for the integration-segregation theory. Moreover, we observed neural interactions between IOR and cognitive conflict, suggesting a potential modulation of conflict processing by attentional orienting. Taken together, these findings provide new insights into exogenous attention by clarifying the neural underpinnings of integration and segregation and uncovering the interaction between spatial orienting and conflict processing.

Keywords: Exogenous attention; inhibition of return; integration-segregation theory; event-related fMRI; cognitive control

Introduction

Attention can be voluntarily directed following one's behavioral goals (goal-directed or endogenous attention) or reflexively oriented by salient information (such as abrupt onsets) in the environment (stimulus-driven or exogenous attention). The exogenous attentional orienting is crucial for efficient visual search in cluttered scenes (Klein et al., 2023; Li et al., 2023; Ma et al., 2011; Wang & Klein, 2010; Wolfe & Horowitz, 2017). Studies employing the cue-target paradigm (Posner & Cohen, 1984) have shown that the exogenous attentional orienting shows a biphasic temporal pattern. An uninformative peripheral cue initially facilitates subsequent target processing at the cued location at short stimulus-onset asynchronies (SOAs), and later turns into inhibiting responses at the cued location at long SOAs (typically over 200 ms), a phenomenon known as inhibition of return (IOR) (Klein, 2000; Lupianez et al., 2006; Posner et al., 1985; Seidel Malkinson et al., 2024). This characteristic shift from facilitation to inhibition at the cued location has fueled decades of theoretical debate, giving rise to multiple competing accounts of its underlying mechanisms (Funes et al., 2008; Klein & Dick, 2002; Lupiáñez, 2010; Lupiáñez et al., 2001; Milliken et al., 2000; Prime & Jolicoeur, 2009; Taylor & Klein, 1998; Vivas et al., 2007).

Among these, one of the most influential and extensively developed theories explaining the biphasic effect is the integration-segregation theory proposed by Lupiáñez and colleagues (Funes et al., 2008; Lupiáñez et al., 2001; Milliken et al., 2000). Rooted in the object file framework (Kahneman et al., 1992), this theory attributes the biphasic

pattern to the dynamic competition between cue-target integration and segregation, two opposing processes. While the integration process favors integrating the targets at the cued locations into an existing episodic representation (an object file) that has been activated by the preceding peripheral cue (Kahneman et al., 1992), the segregation process tends to create a new episodic representation for targets at the uncued locations (Funes et al., 2008; Lupiáñez & Funes, 2005; Lupiáñez et al., 2001; Milliken et al., 2000). At short SOAs (e.g., around less than 250 ms), the integration process in the cued trials is more efficient than the segregation process in the uncued trials, resulting in faster responses for the cued than the uncued trials (i.e., the facilitation effect). At longer SOAs, however, the original object file activated by the cue gradually closed, making it less efficient to integrate new stimuli. Consequently, constructing a new object file at the uncued location gradually becomes easier than updating the closing one, resulting in the IOR effect.

Over the past two decades, the integration-segregation theory has been widely accepted as a flexible and extensible framework for explaining the accumulating IOR research findings (Chen et al., 2007; Funes et al., 2008; Hu et al., 2011; Li et al., 2018; Luo et al., 2010; Lupiáñez et al., 2001; Lupiáñez et al., 2007; Zu et al., 2023), especially showing strengths in explaining the diverse research findings across sensory modalities, feature domains, and task contexts. Originally developed to explain spatial IOR (Funes et al., 2008; Lupiáñez & Funes, 2005; Lupiáñez et al., 2001; Milliken et al., 2000), it has subsequently been extended to nonspatial (e.g., color-, shape-, or frequency-based) IOR in complex

environments (Chen et al., 2007; Hu et al., 2011). When the target and the cue share both non-spatial and spatial features, these consecutive stimuli are integrated into a single event representation, hindering the detection of the target (Chen et al., 2007; Hu et al., 2011). Such integrative interference has also been observed across sensory domains—including the auditory modality—and more recently, in supramodal contexts involving abstract semantic features (Zu et al., 2023). Researchers have further extended the explanatory scope of the integration-segregation framework to electrophysiological data (Li et al., 2018; Martín-Arévalo et al., 2014, 2016). For example, enhanced P3 amplitudes at the uncued locations have been interpreted as reflecting greater cognitive demands associated with new object-file creation underlying IOR (Li et al., 2018), whereas reduced P1 amplitudes at the cued locations have been taken to index a perceptual detection cost arising from disrupted cue-target integration (Martín-Arévalo et al., 2014, 2016).

In addition, the integration-segregation theory also succeeds in accounting for findings that are difficult to explain by other attentional theories, particularly the task-dependent variations in IOR (Chen et al., 2007; Lupiáñez & Milliken, 1999; Lupiáñez et al., 2001; Lupiáñez et al., 2007). According to this framework, the timing of IOR is attributed to task demands, with exogenous orientation being modulated top-down by task relevance. It predicts earlier IOR onsets in detection tasks (favoring an early file closure for new event encoding) and delayed onsets in discrimination tasks (supporting late closure for information accumulation) (Lupiáñez & Milliken, 1999; Lupiáñez et al., 2001). Lupiáñez et al. (2007) further extended this view by showing that, in discrimination tasks,

facilitation for infrequent targets also occurred at long SOAs when IOR for frequent targets took place. This finding is incompatible with the attentional capture and disengagement accounts, and instead suggests cue-target integration dependent on the task set (see also its three-factor extension; Lupiáñez, 2010). In auditory attention research, IOR has also been found to vary with task demands, as task-irrelevant features can either enhance or eliminate the IOR effect depending on whether the cue and target share the same task-relevant dimension (Chen et al., 2007). As reported by Chen et al. (2007), this pattern is better explained by the integration-segregation theory than by the traditional accounts. Collectively, by emphasizing the cue-target interplay, the integration-segregation account provides a comprehensive interpretation of exogenous attention within a unified theoretical framework by incorporating stimulus features, modalities, and task demands.

Despite these strengths, current support for the theory remains largely inferential. Specifically, the hypothesized dual processes of integration and segregation have not been directly evidenced in brain activities. This gap likely reflects that the empirical research had not kept up pace with the theoretical advances, with most of the early neuroimaging work being conducted when the theoretical account of IOR was still evolving and the integration-segregation framework not yet fully formulated. These studies generally assumed that IOR reflects a time-dependent inhibitory state that builds up with the increasing SOA, and that stronger brain activation was expected at longer SOAs regardless of cue validity (Lepsien & Pollmann, 2002; Mayer, Seidenberg, et al., 2004). Following this

assumption, the past studies typically contrasted long and short SOAs to capture the neural dynamics underlying the inhibitory phase of visual attentional orienting, either by collapsing the cued and uncued trials together (Lepsien & Pollmann, 2002; Mayer, Dorflinger, et al., 2004; Müller & Kleinschmidt, 2007; Zhou & Chen, 2008) or by performing the short- vs. long- SOA comparison separately for each cueing condition (Mayer, Seidenberg, et al., 2004). These studies observed the involvement of the frontoparietal attention network, particularly the frontal eye fields (FEF), anterior cingulate cortex (ACC), and inferior parietal lobule (IPL). However, such SOA-based contrasts are insufficient for testing the integration-segregation framework, because they only capture the temporal changes in attentional orienting rather than the functional distinction (integration vs. segregation) that characterizes the theory. To directly test the dual processes of event integration (for the cued targets) and segregation (for the uncued targets), it is necessary to compare the cued and uncued conditions. Some studies did attempt this direct comparison but did not reveal reliable neural differences between the cued and uncued trials during the inhibitory period (Chen et al., 2006; Lepsien & Pollmann, 2002; Mayer, Seidenberg, et al., 2004). For instance, Chen et al. (2006) reported a cue validity effect, but only in the left FEF. The limited neuroimaging evidence for distinct neural responses to the cued and uncued targets in IOR research was likely due to statistical power constraints inherent in event-related functional magnetic resonance imaging (ER-fMRI) experiments (despite their high psychological validity, i.e., estimation efficiency), further aggravated by the suboptimal temporal structure of stimulus

sequences, and the limited sample sizes and trial numbers (Buracas & Boynton, 2002; Liu, 2004; Liu & Frank, 2004; Liu et al., 2001; Wager & Nichols, 2003).

In the current study, we aimed at obtaining direct neuroimaging evidence for the integration-segregation theory employing ER-fMRI with an optimized stimulus sequence following the genetic algorithm (GA) framework (Wager & Nichols, 2003). GA is a class of flexible search algorithms that iteratively optimize sequences based on multiple fitness measures to improve the statistical power of contrast detection while taking into account the estimation efficiency of hemodynamic response function (HRF). According to the integration-segregation theory, targets appearing at the previously cued locations will be engaged by the integration process for an update of the existing cue-activated object file. In contrast, targets appearing at the uncued locations should trigger the segregation process to form a new object file. Therefore, we predicted dissociable neural activations for the cued versus uncued targets. Specifically, we hypothesized that the uncued targets would show a greater engagement of the regions involved in new episodic encoding, such as the parahippocampal gyrus (PHG) (Burgess et al., 2002; Danieli et al., 2023; Hayes et al., 2007; Li et al., 2016; Menon et al., 2000; Torres-Morales & Cansino, 2024), and that the cued targets would show a stronger activation of the regions involved in information integration and attentional reorienting, such as the FEF (Astafiev et al., 2003; Corbetta & Shulman, 2002; Liu et al., 2023).

In addition to the main comparison of the cued vs. uncued locations (i.e., IOR generation mechanisms), we also took the opportunity to investigate the IOR expression

by systematically manipulating the type of target stimuli by varying the color-response key mappings using a Stroop paradigm (De Houwer, 2003; Veen & Carter, 2005; Veen et al., 2001). Three types of stimuli were presented: a neutral condition (non-color words shown in color, producing no conflict), a semantic conflict condition (word meaning and ink color were incongruent, but mapped to the same response), and a combined semantic-response conflict condition (word meaning and ink color were mismatched and mapped to different responses). This design enabled us to examine how spatial attention interacts with distinct levels of cognitive conflict. A previous fMRI study by Chen et al. (2006) reported dissociable neural signatures for the semantic and response conflicts when spatial attention was engaged. Specifically, the increased dorsolateral prefrontal cortex (DLPFC) activity at the cued locations was interpreted within the inhibitory tagging framework as reflecting a temporary disconnection of pre-response representations from response processes. However, that study manipulated response eligibility by excluding certain incongruent color words from the response set (Milham et al., 2001). This method was criticized for conflating the semantic and response conflicts, as ineligible distractors may not be processed in the same way as task-relevant words (Veen & Carter, 2005). To overcome this limitation, the present study adopted an improved Stroop design that clearly separates the semantic and response conflicts (De Houwer, 2003; Veen & Carter, 2005; Veen et al., 2001). This approach provided a more precise test of whether spatial attention differentially modulates these two conflict types and their associated neural mechanisms.

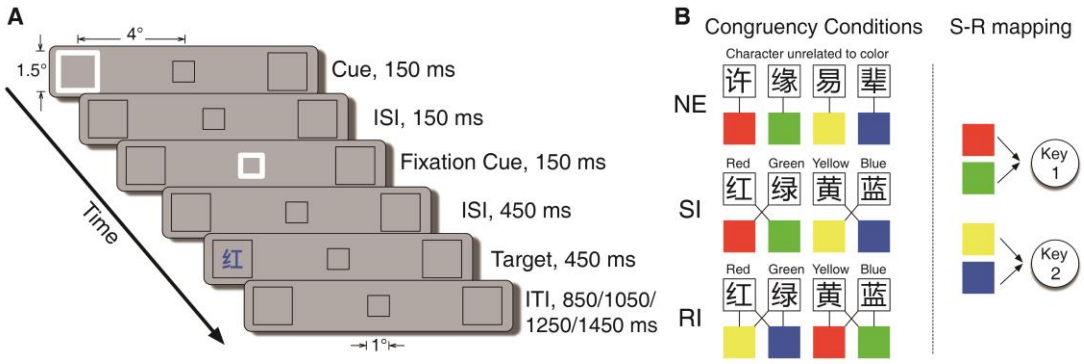

Fig 1. Experimental Materials. A. Trial sequence and display sizes. Each trial starts with a 150-ms non-informative cue at one of the peripheral boxes, followed by a 150-ms fixation cue with a 300-ms SOA. The target was a 450-ms colored Chinese character presented 600 ms after the fixation cue onset at the two target locations with equal probabilities. ISI = interstimulus interval; ITI = intertrial interval. **B.** The character-color combinations in the three congruency conditions. In the neutral condition (first row), the characters were not color-related. In the other conditions, the characters were color names (translation added for illustration purposes). S-R mapping = stimulus-response mapping; NE = neutral; SI = semantically incongruent; RI = response-incongruent.

Results

Participants performed a spatial cueing task (long SOA to elicit IOR) combined with a Stroop paradigm adapted for colored Chinese characters (Chen et al., 2006) (**Fig 1A**), with the characters appearing at either the cued or the uncued location. The experimental manipulation dissociated the semantic and response conflicts, following a well-established three-condition design (**Fig 1B**). These conditions were neutral (NE; non-color characters), semantically incongruent (SI; the character and the color are

incongruent but mapped to the same response, causing only the semantic conflict), and response-incongruent (RI; the character and the color are incongruent and mapped to opposite responses, causing both the semantic and response conflicts) (De Houwer, 2003; Veen & Carter, 2005). Participants responded using two keys, each assigned to two colors. To ensure sufficient statistical power for detecting condition-specific neural differences, the ER-fMRI design was optimized using the Genetic Algorithm (Wager & Nichols, 2003), with the goal of maximizing experimental efficiency for three contrasts of interest. To directly evaluate the prediction of the integration-segregation theory, we first examined the brain activity differences between the conditions of cued-NE (targets at the cued location in the neutral condition) and uncued-NE (targets at the uncued location in the neutral condition). Subsequent analyses examined how IOR modulated the conflict-related neural activities. The contrast of cued-SI minus cued-NE vs. uncued-SI minus uncued-NE was used to assess the effect of IOR on semantic conflict processing, whereas the contrast of cued-RI minus cued-SI vs. uncued-RI minus uncued-SI was employed to capture the modulation of response conflict by IOR.

Behavioral Results

Mean reaction times (RTs) and accuracies are shown in **Fig 2**. **A** two-way (Cue Validity x Congruency) repeated-measures analysis of variance (rm-ANOVA) for the RTs revealed a significant IOR effect (main effect of Cue Validity), $F(1, 28) = 12.057$, $p = .002$, $\eta_p^2 = 0.301$, showing slower responses to targets at the cued location (M = 642 ms, SE = 20 ms) than at the uncued location (632 ± 19 ms). The main effect of Congruency was also significant,

$F(1.53, 42.88) = 29.602$, $p < .001$, $\eta_p^2 = 0.514$ (the Greenhouse–Geisser correction was applied due to the violation of the sphericity assumption). Post hoc comparisons with the Holm-Bonferroni correction (Holm, 1979) revealed significant differences among all conditions (NE vs. RI: $t(28) = -2.179$, $p = .038$, Cohen's $d = 0.071$; NE vs. SI: $t(28) = -5.957$, $p < .001$, Cohen's $d = 0.275$; SI vs. RI: $t(28) = -6.715$, $p < .001$, Cohen's $d = 0.203$), with NE showing the shortest RT (624 ± 19 ms), followed by SI (632 ± 20 ms) then RI (654 ± 21 ms). These data clearly isolated the two distinct conflict effects in the Stroop effect, namely the semantic conflict (SI-NE difference) and the response conflict (RI-SI difference). The interaction did not approach significance, $F(2, 56) = 0.930$, $p = .401$, $\eta_p^2 = 0.032$.

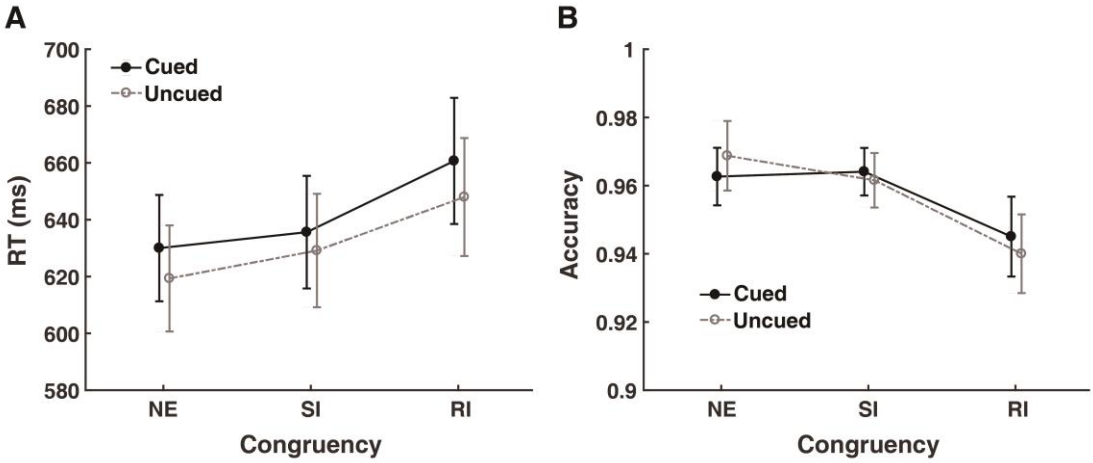

Fig 2. Behavioral Results. Mean reaction times (**A**) and accuracies (**B**) as a function of cue validity and congruency. Error bars extend to one standard error of the mean (SEM).

The rm-ANOVA for the accuracy data (**Fig 2B**) only showed a significant main effect of Congruency, $F(2, 56) = 7.685$, $p = .001$, $\eta_p^2 = 0.215$. Post hoc comparisons confirmed that this came from a lower accuracy in the RI condition ($M = 0.943 \pm SE = 0.009$) than in the NE (0.966 ± 0.009; $t(28) = -3.596$, $p = .002$, Cohen's $d = 0.446$) and SI (0.963 ± 0.009;

$t(28) = -3.150$, $p = .005$, Cohen's $d = 0.391$) conditions. No significant difference was found between the NE and SI conditions ($t(28) = 0.446$, $p = .657$, Cohen's $d = 0.055$). The main effect of Cue Validity ($F(1, 28) = 0.021$, $p = .887$, $\eta_p^2 < 0.001$) and the interaction ($F(2, 56) = 1.298$, $p = .281$, $\eta_p^2 = 0.044$) were not significant. No speed-accuracy trade-off was noticed in the current data.

Neuroimaging Results

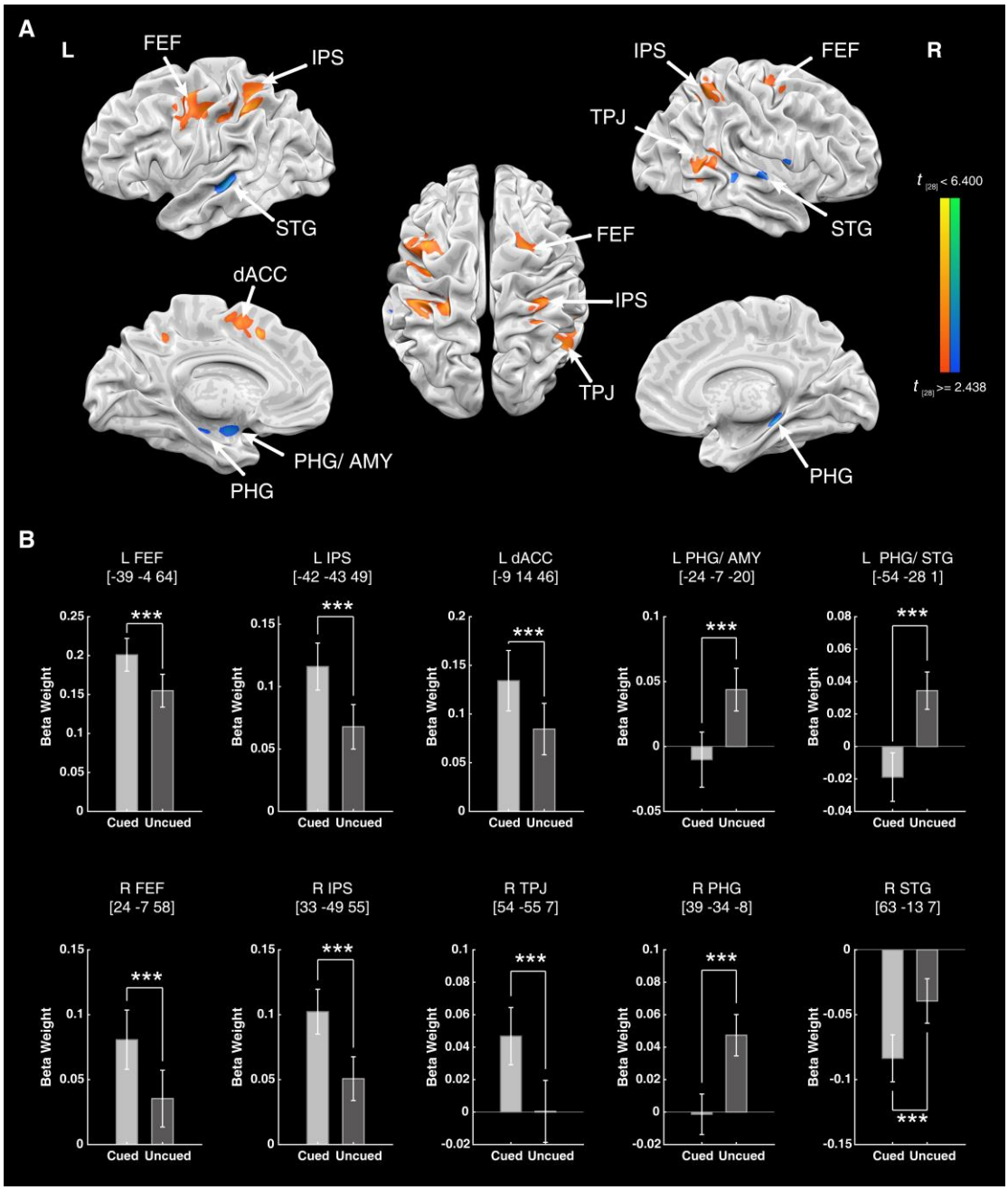

Fig 3. IOR Effect in the Neutral Condition and Parameter Estimation. A. Brain regions showing significant activations in the contrast between the cued-NE and uncued-NE conditions, with a threshold of $p < 0.005$ (uncorrected) with a minimum cluster size of 540 mm^3 (20 voxels), yielding a corrected $p < 0.05$ based on 2,500 Monte Carlo simulations in BrainVoyager. Warm colors

represent stronger activations in the cued condition, and cold colors represent stronger activations in the uncued condition. **B.** Parameter estimates for each activation region. Error bars extend to 1 SEM. L = left; R = right. *** $p < .001$.

IOR Effect in the Neutral Condition

The contrast between the cued-NE and uncued-NE conditions was examined to identify the underlying neural mechanisms of the IOR effect during the processing of neutral targets. Whole-brain fMRI findings revealed two distinct activation patterns in response to these conditions (**Fig 3A**). Relative to the uncued-NE condition, the cued-NE condition showed enhanced activations in the dorsal attention network (DAN) including the bilateral FEF and IPS, along with the right-lateralized TPJ from the ventral attention network (VAN), and the left dACC. In contrast, the uncued-NE condition demonstrated stronger activations in the bilateral PHG and STG than the cued-NE condition. To further compare the activity levels in each brain region between the cued-NE and uncued-NE conditions, paired *t*-tests were conducted on the average parameter estimates (beta weights) in the left and right IPS, FEF, PHG, and STG, as well as the left dACC and right TPJ (all *p*s < .001, see **Fig 3B**). Detailed information on the activated regions' coordinates, cluster sizes, and statistical significance is provided in Table 1.

Table 1. Brain regions showing significant activation differences between the cued-NE and uncued-NE conditions.

Regions	Laterality	Cluster (voxels)	MNI coordinates peak			T_{max}	T_{mean}	BA
			x	y	Z			
Frontal Eye Field	L	146	-39	-4	64	4.51	3.43	6
	R	28	24	-7	58	4.32	3.52	6
Intraparietal Sulcus	L	120	-42	-43	49	4.73	3.57	40
	R	82	33	-49	55	5.12	3.78	40
Dorsal Anterior Cingulate Cortex	L	36	-9	14	46	5.05	3.46	32
Temporoparietal Junction	R	75	54	-55	7	4.23	3.45	39
Parahippocampal Gyrus	L	22	-24	-7	-20	-4.11	-3.46	/
	R	44	39	-34	-8	-5.44	-3.83	/
Parahippocampal Gyrus/ Superior Temporal Gyrus	L	84	-54	-28	1	-4.42	-3.49	21
Superior Temporal Gyrus	R	32	63	-13	7	-4.22	-3.48	22

BA = Brodmann area; L = left; R = right.

Effect of IOR on Semantic Conflict

Although the IOR effect showed no effect on either the semantic conflict difference (SI-NE) or the response conflict difference (RI-SI) in the behavioral performance, differential neural activities were observed between these conditions (summarized in **Fig 4** and **Table 2**). The effect of IOR on the semantic conflict was examined as the contrast between

the SI-NE differences (SI minus NE) in the cued and the uncued conditions. As illustrated in **Fig 4A**, the right dACC showed significantly reduced activation. A two-way rm-ANOVA was conducted on the average parameter estimates (beta weights) obtained from these contrasts for each activated region. The results confirmed a significant interplay between semantic conflict and IOR in the right dACC, $F(1,28) = 15.946$, $p < .001$, $\eta_p^2 = 0.363$. Greater neural activities were found in the SI condition compared to the NE condition when the targets were presented at the uncued location ($t(28) = 3.262$, $p = .003$, Cohen's $d = 0.606$), but not for the targets at the cued location ($t(28) = -1.010$, $p = .321$, Cohen's $d = 0.187$).

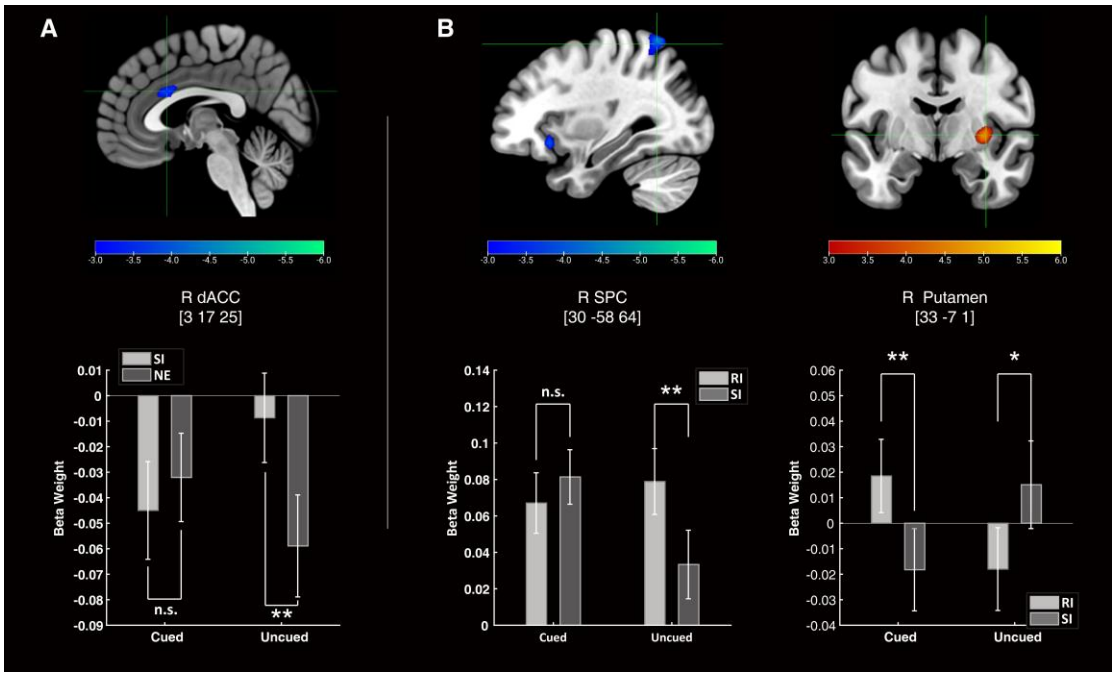

Fig 4. IOR Effect under the Semantic Conflict (A) and the Response Conflict (B). These two effects were quantified as cued-SI minus cued_NE > uncued-SI minus uncued-NE and cued-RI minus cued-SI > uncued-RI minus uncued-SI, respectively. Parameter estimations were based on a threshold of $p < 0.005$ (uncorrected), with a minimum cluster size of 540 mm^3 (20 voxels), yielding

a corrected $p < 0.05$ based on 2500 Monte Carlo simulations in BrainVoyager. Error bars extend to 1 SEM. $^{**}p < .01$, $^{*}p < .05$, n.s. = non-significant.

Effect of IOR on Response Conflict

To explore the influence of IOR on response conflict, we compared the cued (RI–SI) and the uncued (RI–SI) conditions (**Fig 4B** and **Table 2**). The right superior parietal cortex (SPC) showed a significant activation reduction (**Fig 4B, left)**, while the right putamen exhibited an activation enhancement (**Fig 4B, right**). A two-way rm-ANOVA on the beta weights revealed a significant interaction in the right SPC, $F(1,28) = 20.833$, $p < .001$, $\eta_p^2 = 0.427$. Specifically, it showed greater activations in the RI condition compared to the SI condition when the targets were presented at the uncued location ($t(28) = 3.447$, $p = .002$, Cohen's $d = 0.640$), but not for the cued location ($t(28) = -0.962$, $p = .344$, Cohen's $d = 0.179$).The right putamen also demonstrated a significant interaction ($F(1,28) = 26.686$, $p < .001$, $\eta_p^2 = 0.488$), but with a different pattern. The activation was stronger in the RI than the SI conditions for the cued location ($t(28) = 2.983$, $p = .006$, Cohen's $d = 0.554$); and the opposite pattern was observed for the uncued location ($t(28) = -2.404$, $p = .023$, Cohen's $d = 0.446$).

Table 2. Brain regions showing a significant modulation effect of IOR on semantic conflict (cued-SI minus cued_NE > uncued-SI minus uncued-NE) or response conflict (cued-RI minus cued-SI > uncued-RI minus uncued-SI).

Region	Laterality	Cluster (voxels)	MNI coordinates peak			T_{max}	T_{mean}	BA
			x	y	z			
Effect of IOR on Semantic Conflict								
Dorsal Anterior Cingulate Cortex	R	24	3	17	25	-3.78	-3.34	24
Effect of IOR on Response Conflict								
Superior Parietal Cortex	R	67	30	-58	64	-4.74	-3.49	7
Putamen	R	31	33	-7	1	4.91	3.80	/

BA = Brodmann area; R = right.

Discussion

The integration-segregation theory has emerged as an influential framework for explaining the dynamic effects of exogenous attention (Chen et al., 2007; Funes et al., 2008; Hu et al., 2011; Li et al., 2018; Lupiáñez et al., 2001; Lupiáñez et al., 2007; Zu et al., 2023), attributing the turning from the early attentional facilitation to the later IOR to the dynamic processes of cue-target integration and segregation (Funes et al., 2008; Lupiáñez & Funes, 2005; Lupiáñez et al., 2001; Milliken et al., 2000). In the current study, by contrasting the cued versus the uncued targets, we provided the first direct neuroimaging evidence supporting this theory by dissociating brain activation patterns associated with these two processes. Stronger responses were found in the bilateral FEF, IPS, right TPJ,

329 and left dACC in the cued than the uncued targets. Relative to the cued targets, the uncued
330 targets showed stronger activations in the bilateral PHG and STG.

331 The heightened activation observed for targets appearing at the cued locations
332 (particularly in the bilateral FEF, IPS, and right TPJ) reflects the attentional demand
333 associated with the integration process. According to the integration-segregation theory
334 (Funes et al., 2008; Lupiáñez & Funes, 2005; Lupiáñez et al., 2001; Milliken et al., 2000),
335 the cue-initiated object file is likely to have closed or begin closing under the long SOA
336 conditions, hindering immediate integration of the subsequent targets. To integrate a
337 target appearing again at the cued location, the object file needs to be reopened with
338 reallocation of attentional resources. Our neuroimaging data captured this process by
339 showing coordinated activation in the bilateral FEF and IPS (key nodes of the dorsal
340 attention network) and in the right TPJ (a core region of the ventral attention network)
341 (Ahrens et al., 2019; Corbetta & Shulman, 2002; Fox et al., 2006; Vossel et al., 2014). These
342 regions act in concert to support the attentional shifts and reorienting necessary for
343 reopening the object file for integration. Additionally, the observed increase in left dACC
344 activity under the cued relative to the uncued condition likely reflects the engagement of
345 cognitive control mechanisms (Botvinick et al., 2004; Chung et al., 2024; Mayer et al., 2012;
346 Veen & Carter, 2005) to resolve the difficulty with the task-driven requirement of target
347 integration facing the reduced accessibility of the cue-initiated representation. It is also
348 possible that the heightened activation of dACC represents the inhibitory bias toward the
349 direction of the cued location (Mayer, Seidenberg, et al., 2004).

350 In contrast, the stronger activation in the uncued condition was observed in the
351 bilateral PHG extending into the STG. Located in the medial temporal lobe surrounding
352 the hippocampus, the PHG is critically involved in episodic encoding, particularly for
353 novel visual or spatial stimuli (Burgess et al., 2002; Danieli et al., 2023; Hayes et al., 2007;

Li et al., 2016; Menon et al., 2000; Torres-Morales & Cansino, 2024). In our task, the targets appearing at the uncued locations likely represented novel events requiring new spatial registration. Following the theorized segregation process, such events require the creation of new object files (Kahneman et al., 1992) by engaging brain regions involved in novelty detection and contextual updating. The enhanced PHG/STG activities observed in the uncued condition may reflect the encoding of new spatial representations of the segregation process.

Our data provided clear support for the integration-segregation theory. It is also noteworthy that, although prior studies investigated the neural mechanisms of IOR (Bourgeois et al., 2013a, 2013b; Hanlon et al., 2017; Lepsien & Pollmann, 2002; Mayer, Dorflinger, et al., 2004; Mayer et al., 2007; Mayer, Seidenberg, et al., 2004; Müller & Kleinschmidt, 2007; Satel et al., 2019; Yang & Mayer, 2014; Zhou & Chen, 2008), none identified distinct activation patterns corresponding to the integration and segregation processes as in our data. Specifically, most of the previous IOR studies did not show significant brain activations when contrasting the cued and uncued conditions (Lepsien & Pollmann, 2002; Mayer, Seidenberg, et al., 2004), except Chen et al. (2006) reported a cue-validity effect confined to the left FEF. Instead, some indirect approaches, such as comparing long- and short-SOA trials while collapsing over the cueing conditions, reported activations in regions like the FEF, TPJ, ACC, and posterior parietal cortex (Lepsien & Pollmann, 2002; Mayer, Dorflinger, et al., 2004; Mayer, Seidenberg, et al., 2004; Müller & Kleinschmidt, 2007; Zhou & Chen, 2008), showing some similarity with the integration-related network observed in the current study. However, the findings were inconsistent across studies, with some reporting only a limited subset of regions and others showing lateralized instead of bilateral effects (e.g., stronger right-hemisphere FEF activation; Lepsien & Pollmann, 2002; Mayer, Dorflinger, et al., 2004). Similar frontoparietal engagement has also been observed in auditory and cross-modal IOR

380 studies (Hanlon et al., 2017; Mayer et al., 2009; Mayer et al., 2007; Yang & Mayer, 2014),
381 typically present across various SOAs (e.g., sustained activation in both the dorsal and
382 ventral frontoparietal regions regardless of SOA length; Hanlon et al., 2017) or showing
383 SOA-dependent effects (e.g., reversed direction of activation differences between short
384 and long SOAs; Mayer et al., 2007). Complementing these observations, transcranial
385 magnetic stimulation (TMS) studies have provided causal evidence for the contribution
386 of frontoparietal regions in IOR (Bourgeois et al., 2013a, 2013b; Chica et al., 2011; Ro et
387 al., 2003). For instance, stimulation over the right FEF during the cue-target interval has
388 been shown to eliminate the typical IOR effect for the cued targets in the ipsilateral
389 hemifield (Ro et al., 2003). Similarly, TMS applied to the right IPS/TPJ also disrupted the
390 IOR effect (Bourgeois et al., 2013a; Chica et al., 2011), whereas stimulation over their left-
391 hemisphere counterparts did not cause much change in IOR (Bourgeois et al., 2013b).
392 These findings suggest a possible right-lateralized neural organization of the integration
393 process. However, this lateralization notion conflicts with the largely bilateral activation
394 pattern observed in our study. The lack of systematic testing for the left-hemisphere
395 contribution in previous TMS studies leaves this asymmetry open to further investigation.
396 Notably, despite offering partial (and often lateralized) support for the integration
397 process, none of these prior studies have addressed the neural mechanisms underlying
398 the segregation process, which is uniquely revealed by the present neuroimaging findings.

399 The above discrepancies between our findings and the previous studies may stem
400 from several methodological and design factors. Firstly, the prior studies likely
401 introduced confounds when investigating IOR indirectly. When comparing long and short
402 SOAs, the observed effects may have been jointly influenced by factors unrelated to IOR,
403 such as working memory (i.e., increased demand of maintaining the cue representation
404 over longer intervals; Mayer et al., 2007) and temporal attention (i.e., distinct temporal

expectations formed by variations in SOA; Nobre & van Ede, 2018). Moreover, the IOR effect depends not only on cue-induced attentional orienting, but also on the dynamic interaction between the target onset and the ongoing cue-related neural activity (Lupiáñez, 2010; Nobre & van Ede, 2018; Taylor & Donnelly, 2002). These confounds could potentially obscure the genuine IOR effect. Secondly, differences in statistical power may also account for the discrepancies. In the present study, we employed an optimized GA stimulus sequence (Wager & Nichols, 2003), which provides greater statistical power than simple random sequences while maintaining a high estimation efficiency (for details, see the Methods and Supplementary Information sections). This optimization likely enhanced the reliability of the estimated neural responses (Wager & Nichols, 2003). In addition, the previous neuroimaging studies on IOR often relied on relatively small sample sizes (around 10-12 participants; Chen et al., 2006; Mayer, Dorflinger, et al., 2004; Mayer, Seidenberg, et al., 2004; Müller & Kleinschmidt, 2007) or a limited number of trials (e.g., 30 trials per condition; Lepsien & Pollmann, 2002), leading to much reduced statistical power and a higher probability of false negatives. In contrast, the current study increased both the number of trials and the sample size, having effectively enhanced the sensitivity of detecting differences between experimental conditions (Baker et al., 2021; Chen et al., 2022). Finally, task design differences may further contribute to the observed inconsistencies. The earlier studies often employed simple localization or detection tasks (Lepsien & Pollmann, 2002; Mayer, Dorflinger, et al., 2004; Mayer, Seidenberg, et al., 2004; Müller & Kleinschmidt, 2007), while the current study adopted a discrimination task. According to the integration-segregation theory (Funes et al., 2008; Lupiáñez & Funes,

427 2005; Lupiáñez et al., 2001; Lupiáñez et al., 2007; Milliken et al., 2000), more complex
428 stimuli may require greater cognitive resources to establish object files, leading to
429 enhanced processing of object files and heightened detectability of the underlying
430 integration and segregation processes.

431 Another novelty of the current study is integrating the IOR and the modified Stroop
432 tasks, which separately studied semantic- and response-level conflicts (De Houwer, 2003;
433 Veen & Carter, 2005). Through this design, we made an additional discovery about how
434 IOR modulates the ongoing Stroop interference effect at the inhibited (i.e., cued) locations.
435 Behaviorally, our results showed no significant interaction between IOR and any conflict
436 in the Stroop task, not replicating the previous findings (Chen et al., 2006; Vivas & Fuentes,
437 2001) of reduced Stroop interference at the cued relative to the uncued locations. Yet, at
438 the neural level, the brain regions involved in conflict processing were engaged in the
439 interaction between IOR and the Stroop effect. Specifically, the right dACC, which is
440 involved in semantic conflict processing (Li et al., 2017; Milham et al., 2001; Veen & Carter,
441 2005), appeared to serve as a critical neural interface for the interaction between
442 semantic conflict and IOR. Specifically, in the uncued condition, the semantic
443 incongruency elicited stronger activations compared to the neutral condition, a pattern
444 that disappeared or even reversed in the cued condition. Regarding the interaction
445 between response conflict and IOR, brain regions such as the right SPC, which are
446 involved in detecting response conflict and orienting spatial attention (Li et al., 2017),
447 played a key role. Similarly, this region exhibited stronger conflict effects (i.e., greater

activation in the RI than SI condition) in the uncued condition compared to the cued condition. These results can be interpreted by the inhibitory tagging mechanism proposed by Fuentes et al. (1999), which posits that, when attention is drawn away from a cued location, stimuli presented there are temporarily tagged with inhibition (Fuentes et al., 2000; Fuentes et al., 1999; Vivas & Fuentes, 2001). ERP evidence supporting this mechanism was reported by Zhang et al. (2012), who showed that the Stroop conflict-related N450 effects were delayed and attenuated at the cued compared to the uncued locations, suggesting a temporary disruption of the stimulus-response link. Such inhibitory tagging may attenuate or even disrupt conflict processing at the inhibited location, offering a plausible account for the neural interactions between IOR and Stroop conflicts observed in our study. The current results could also potentially suggest that the effects of inhibitory tagging are not limited to stimulus-response connections (as proposed by Fuentes et al., 1999), but also extend to semantic representations, as evidenced by the modulation of the right dACC observed in our study. This notion is consistent with a previous finding that the N400 ERP component (a biomarker of semantic processing) had a decreased amplitude for the cued position (Zhang & Zhang, 2007). This highlights that spatial attention can affect subsequent cognitive processes at the semantic level (Cristescu & Nobre, 2008; Zhang & Zhang, 2007).

Furthermore, we observed pronounced neural responses in the right putamen when contrasting the RI and SI conditions at the cued versus the uncued locations. The putamen is a subcortical nucleus in the basal ganglia and has been found to be involved in control

469 of response interference (Schmidt et al., 2018; Schmidt et al., 2020). For example, Schmidt
470 et al. (2020) demonstrated that the dorsal striatum, including the putamen, is engaged
471 during Simon-type interference by supporting task-appropriate response selection and
472 suppression of competing alternatives, and that its damage leads to less efficient
473 interference control (Schmidt et al., 2018). These findings support the view that the
474 putamen is recruited when interference arises at the response-selection level. Building
475 on this, we speculated that the enhanced putamen activation in the cued conditions in the
476 current study reflects an increased demand for response control when attentional
477 resources were reduced by IOR. Taken together, our findings highlight a potential neural
478 basis for the interaction between IOR and conflict processing encompassing both
479 semantic and response domains.

480 However, these results should be interpreted with caution given the absence of
481 behavioral support. One potential explanation of this dissociation is the usage in the
482 current study of the GA-optimized sequence, which prioritizes both detection and HRF
483 estimation efficiency. This optimization made the event order converging towards a
484 block-like structure, thereby having reduced event counterbalancing and increased
485 sequential predictability (Wager & Nichols, 2003). Such unintended regularities may have
486 influenced participants' behavioral strategies (e.g., forming expectations about upcoming
487 events), thereby weakening the correspondence between the neural and behavioral
488 findings. Future studies should address this limitation by employing more optimized
489 designs that consider some psychological factors (e.g., event counterbalancing; Wager &

Nichols, 2003) to better validate the observed neural mechanisms. Alternatively, the observed neural-behavioral response dissociation may reflect differences in measurement sensitivity between the neural and behavioral indices (Chen et al., 2006; Wilkinson & Halligan, 2004). A similar pattern of dissociation was reported by Chen et al. (2006), who found that the response conflict was not modulated by IOR behaviorally, yet the regions associated with conflict resolution exhibited stronger activations in the cued condition. As noted by Wilkinson and Halligan (2004), RTs and accuracies are not perfect measures of cognition, whereas neural signals can reveal finer-grained or "hidden" processes that precede overt behavior. Thus, neural modulations may emerge even in the absence of detectable behavioral differences.

In conclusion, the current study provides the first direct neuroimaging evidence lending support to the hypothesis of the integration–segregation theory (Funes et al., 2008; Lupiáñez & Funes, 2005; Lupiáñez et al., 2001; Milliken et al., 2000). We revealed distinct neural mechanisms for processing of the cued and uncued targets during IOR, with attentional integration engaging the frontoparietal attention network (FEF, IPS, TPJ, dACC) and segregation recruiting the medial temporal regions (PHG–STG) associated with new object-file formation and novelty encoding. These dissociated activations offered direct support for the dynamic interplay between the integration and segregation processes. We also identified interactions between IOR and cognitive conflict in brain activities, suggesting that attentional orienting can modulate conflict processing at both the semantic and response levels. Taken together, our findings revealed the neural

underpinnings of the integration-segregation theory and advanced our understanding of the neural mechanisms linking exogenous attentional orienting and cognitive control.

Methods

Participants

32 healthy participants with normal or corrected-to-normal vision and normal color vision were recruited. None reported a history of neurological disorders. Data from three participants were excluded due to excessive head movements and high global variances (see fMRI Data Analysis), leaving 29 participants for analysis (18 female, 11 male; mean age ± SD = 22.69 ± 2.58 years). All participants were naïve to the purpose of the study, provided written informed consent approved by the Ethics Committees of Northeast Normal University and Soochow University, and received monetary compensation. The sample size was informed by a power analysis using MorePower 6.0 (Campbell & Thompson, 2012) for a within-subjects rm-ANOVA. To achieve an 80% statistical power at the threshold of $\alpha = .05$ (Chen et al., 2006), 14 participants were required. In addition, we also acknowledged that effect sizes from published studies are often inflated due to the publication bias (Albers & Lakens, 2018). To mitigate this potential risk, we determined to acquire data from a sample sized at least double of the suggested size by the power analysis (i.e., $N \geqslant 28$).

Experimental Design

The experiment adopted a within-subjects design with two factors, namely Cue Validity (cued vs. uncued) and Congruency (SI, RI, and NE). The targets appeared at the cued location in the cued trials and at the other peripheral location in the uncued trials. The congruency factor referred to the relationship between the color and meaning of the Chinese characters (i.e., targets). In total, eight characters and four colors were used (see

Fig 1B). In an SI trial, the color and character meaning differed but were mapped to the same response key (e.g., character "红" ["red"] displayed in green, which was related to the same response key). In an RI trial, the color and character meaning differed and were mapped to different response keys (e.g., "红" displayed in yellow, which was related to another key). The NE trials used characters that were not related to color in the meanings and shared the same orthographic structures (character complexity and form) of the color-meaning characters. In addition to the six experimental conditions, we added a null condition, in which no Chinese character was shown, to increase the statistical power of detecting differences across conditions (Friston et al., 1999).

It is worth noting that the statistical power of effects in rapid ER-fMRI depends greatly on specific sequences of stimulus events (Liu & Frank, 2004; Wager & Nichols, 2003). To ensure high design efficiency, we optimized the stimulus sequences employing the genetic algorithm (see Supplementary Information for details) (Wager & Nichols, 2003). This optimization improves the detection efficiency for the contrasts of interest by moderately sacrificing the efficiency of less relevant contrasts (Wager & Nichols, 2003). In the current study, we focused on three contrasts, including cued-NE vs. uncued-NE, cued-SI minus cued-NE vs. uncued-SI minus uncued-NE, and cued-RI minus cued-SI vs. uncued-RI minus uncued-SI. These contrasts respectively examined the IOR effect, the modulation of semantic conflict processing by IOR, and the modulation of response conflict processing by IOR. The optimized sequences were used for all but two participants, whose trial sequences were constructed using a truncated M-sequence (Buracas & Boynton, 2002) implemented in an earlier version of the experiment.

Stimuli and Procedure

Each participant completed two functional scans (i.e., experimental runs) and one anatomical scan in a single session. Each experimental run employed a rapid event-

related design and had each of the seven conditions (six experimental conditions plus the null condition) repeated 48 times (336 trials per run). Across the two runs, this yielded a total of 672 trials (96 trials per condition).

All trials displayed a three-box display over a gray background, including a central black fixation box (1°×1°, line width of 0.02°) and two black placeholder boxes (1.5°×1.5°, line width of 0.02°) positioned 4° (center-to-center) to the left and right of the fixation box. Each run began and ended with this display for 16 and 20 s, respectively. The trial sequence is illustrated in **Fig 1A**. In a null trial, only the three boxes were shown for the trial duration. In any of the six experimental conditions, each trial started with one of the peripheral boxes changing to a white color with a line width of 0.05° for 150 ms to attract attention to this peripheral location (cue). 150 ms after the offset of the peripheral cue, the central fixation box turned into white with a line width of 0.05° for 150 ms to force attention back to the central location (central cue). After another 450 ms, a colored Chinese character (in the STSong font, 1.4°×1.4°) was presented (target) for 450 ms inside one of the two peripheral boxes with equal probabilities. Participants were required to ignore the meaning of the character and identify the word color as quickly and accurately as possible by pressing one of the two keys designated for the color categories (red/green and blue/yellow) with their middle and index fingers, respectively (**Fig 1B**). The color category-button mapping was counterbalanced across participants. Furthermore, to avoid a possible occurrence of the Simon effect (Klein & Ivanoff, 2011), the response keys were vertically arranged. Each trial ended with an inter-trial interval (ITI) with a duration of 850, 1,050, 1,250, or 1,450 ms (randomized with equal probabilities). The average trial duration was 2,500 ms.

Before the scanning, all participants had two practice parts outside the scanner to familiarize themselves with the task and the stimuli. In the first part, the participants practiced on a discrimination task with only color patches (no Chinese characters) using

the predefined color category-button mapping. Once having reached an accuracy of 96%, the participants did the second part and completed 24 practice trials of the experimental task as in the scanning runs.

Apparatus and Data Acquisition

The imaging data were acquired at two research sites following comparable protocols. At the Imaging Center for Brain Research of Beijing Normal University, the stimuli were presented with E-Prime (Psychological Software Tools, Pittsburgh, PA) on an LCD monitor (1024×768 resolution, 60 Hz refresh rate) viewed through a head-coil-mounted mirror (115 cm optical distance). The data were collected using a Siemens 3-Tesla Tim Trio scanner with a head coil. The functional data were acquired through a T2*-weighted echo planar imaging (EPI) sequence (TR = 2,000 ms; TE = 30 ms; flip angle = 90°; FOV = 220×220 mm; matrix size = 64×64). Thirty-three transversal slices covering the whole brain (slice thickness = 4 mm; in-plane resolution = 3.44×3.44 mm; slice gap = 0.4 mm) were acquired in an interleaved ascending order. Each participant completed two functional runs of 400 volumes (including 8 initial dummy volumes). High-resolution anatomic images were collected using a T1*-weighted magnetization-prepared rapid gradient echo (MP-RAGE) sequence consisting of 128 sagittal slices (TR = 2,300 ms; TE = 3.9 ms; flip angle = 8°; FOV = 256×256 mm, matrix size = 256×256, voxel resolution = 1.33×1×1 mm, slice gap = 0 mm).

At the Imaging Center of the First Affiliated Hospital of Soochow University, the stimuli were presented with MATLAB (The MathWorks, Natick, MA) and the Psychophysics Toolbox (Brainard, 1997) on a monitor (also 1920×1080 and 60 Hz) viewed through a mirror at an optical distance of 251 cm. The imaging data were recorded using a 3-Tesla Philips Ingenia scanner equipped with a head coil. The functional images featured a matrix size of 80×80, an in-plane resolution of 2.75×2.74 mm, and no slice gap.

611 The structural images were acquired with a voxel resolution of 1×1×1 mm across 180
612 slices (FOV = 240×240 mm; matrix size = 240×240). The other parameters remained the
613 same as those used at Beijing Normal University.

614 Data Analysis

615 **Behavioral analysis.** Trials with incorrect responses and RTs shorter than 100 ms or
616 longer than 1,300 ms (5.52% of total trials) were excluded from statistical analyses. Mean
617 RTs on correct trials and response accuracies were entered into the two-way rm-ANOVA.

618 **fMRI Data Analysis.** The fMRI preprocessing and analysis were conducted with the
619 BrainVoyager QX (version 2.2, Brain Innovation) software package(Goebel et al., 2006).
620 The initial eight functional volumes of each scan were discarded to allow signal
621 equilibration. For the remaining functional images, slice timing correction was applied
622 using sinc interpolation, followed by 3D motion correction with trilinear/sinc
623 interpolation for intra-session alignment to the middle volume. Each run for each
624 participant was examined for the six head motion parameters (three rotations and three
625 translations). Runs with motions exceeding one voxel length in any direction were
626 excluded. An isotropic Gaussian kernel of an 8-mm full width at half maximum (FWHM)
627 was then applied to spatially smooth the images. Finally, linear trend removal was
628 performed, along with high-pass temporal filtering at a cutoff of approximately 0.0081 Hz
629 (corresponding to seven cycles per run), to remove low-frequency nonlinear drifts. After
630 these steps, we checked the variance in the global signals to assess the data quality,
631 specifically for detection of any abrupt changes in the time course of each run. Volumes
632 containing abrupt changes were interpolated, and runs exhibiting a global variance
633 exceeding 0.1% were excluded. For each participant, the accepted fMRI data were co-
634 registered with an anatomical scan in the native space and further transformed to the

standard Montreal Neurological Institute (MNI) 152 space, with a resampled voxel size of 3×3×3 mm.

After the preprocessing, statistical analyses were performed using a random effects general linear model (RFX-GLM) analysis within BrainVoyager, executing a multi-subject GLM with distinct predictors for each participant. Using a deconvolution and multiple regression approach, we modeled six experimental conditions and one "error" term (including all the error trials) for each participant, with each condition including six sampling points taken from the 0-12 s period after the cue presentation (i.e., one sampling point every 2 seconds). The functional images occurring 5-10 s after the cue onsets, corresponding to the peak of the hemodynamic response function (HRF, Cohen, 1997), were used to provide parameter estimates for the amplitudes of the HRF. Volumes deviating in intensity by ±3 SDs or more from the individual means were removed by a weighted vector that was included in the model as a covariate of no interest. In addition, the six mean-centered head motion parameters were modeled as covariates of no interest to further remove any residual variance due to head motion. To mitigate noise related to global physiological processes, the model incorporated the global signal, which represented the normalized average activity across all voxels at each time point in the standard space, as an additional predictor. We examined the three contrasts of interest introduced earlier. Corrections for multiple comparisons at $p < 0.05$ were made through the Cluster Threshold plugin (BrainVoyager) using 2,500 Monte Carlo simulations. Minimum cluster sizes (540 mm^3 corresponding to 20 voxels) corresponding to significance at a threshold of $p < 0.005$ (uncorrected) were computed for each contrast (Forman et al., 1995). The approximate Brodmann areas (BAs) and the corresponding anatomical labels of the peak voxel of the significant clusters in the MNI space were identified using the Neuroelf toolbox v1.1 (Weber, 2017).

Data Availability

The processed data used for the final analyses are available at https://github.com/yangzhangpsy/ER-fMRI-IOR. Raw data for this study can be requested from the Lead Contact, and the authors confirm that all reasonable requests will be fulfilled.

Declaration of Competing Interest

The authors declare no conflicts of interest for the publication of this article.

Acknowledgments

This research was supported by grants from the Brain Science and Brain-like Intelligence Technology-National Science and Technology Major Project (2025ZD0215702), the National Natural Science Foundation of China (32171049), the Social Science Foundation of Jiangsu Province (22JYB015), the China Postdoctoral Science Foundation (2024M752310), and Jiangsu Funding Program for Excellent Postdoctoral Talent (2024ZB496, 2025ZB642).

References

Ahrens, M., Veniero, D., Freund, I. M., Harvey, M., & Thut, G. (2019). Both dorsal and ventral attention network nodes are implicated in exogenously driven visuospatial anticipation. *Cortex*, *117*, 168-181. https://doi.org/10.1016/j.cortex.2019.02.031

Albers, C., & Lakens, D. (2018). When power analyses based on pilot data are biased: Inaccurate effect size estimators and follow-up bias. *Journal Of Experimental Social Psychology*, *74*, 187-195. https://doi.org/10.1016/j.jesp.2017.09.004

Astafiev, S. V., Shulman, G. L., Stanley, C. M., Snyder, A. Z., Van Essen, D. C., & Corbetta, M. (2003). Functional organization of human intraparietal and frontal cortex for attending, looking, and pointing. *Journal of Neuroscience*, *23*(11), 4689-4699. https://doi.org/10.1523/jneurosci.23-11-04689.2003

Baker, D. H., Vilidaite, G., Lygo, F. A., Smith, A. K., Flack, T. R., Gouws, A. D., & Andrews, T. J. (2021). Power contours: Optimising sample size and precision in experimental psychology and human neuroscience. *Psychological Methods*, *26*(3), 295-314. https://doi.org/10.1037/met0000337

Botvinick, M. M., Cohen, J. D., & Carter, C. S. (2004). Conflict monitoring and anterior cingulate cortex: An update. *Trends in Cognitive Sciences*, *8*(12), 539-546. https://doi.org/10.1016/j.tics.2004.10.003

Bourgeois, A., Chica, A. B., Valero-Cabré, A., & Bartolomeo, P. (2013a). Cortical control of inhibition of return: Causal evidence for task-dependent modulations by dorsal and ventral parietal regions. *Cortex*, *49*(8), 2229-2238. https://doi.org/10.1016/j.cortex.2012.10.017

Bourgeois, A., Chica, A. B., Valero-Cabré, A., & Bartolomeo, P. (2013b). Cortical control of Inhibition of Return: Exploring the causal contributions of the left parietal cortex. *Cortex*, *49*(10), 2927-2934. https://doi.org/10.1016/j.cortex.2013.08.004

Brainard, D. H. (1997). The Psychophysics Toolbox. *Spatial Vision*, *10*(4), 433-436. https://doi.org/10.1163/156856897x00357

Buracas, G. T., & Boynton, G. M. (2002). Efficient design of event-related fMRI experiments using M-sequences. *NeuroImage*, *16*(3 Pt 1), 801-813. https://doi.org/10.1006/nimg.2002.1116

Burgess, N., Maguire, E. A., & O'Keefe, J. (2002). The human hippocampus and spatial and episodic memory. *Neuron*, *35*(4), 625-641. https://doi.org/10.1016/S0896-6273(02)00830-9

Campbell, J. I. D., & Thompson, V. A. (2012). MorePower 6.0 for ANOVA with relational confidence intervals and Bayesian analysis. *Behavior Research Methods*, *44*(4), 1255-1265. https://doi.org/10.3758/s13428-012-0186-0

Chen, G., Pine, D. S., Brotman, M. A., Smith, A. R., Cox, R. W., Taylor, P. A., & Haller, S. P. (2022). Hyperbolic trade-off: The importance of balancing trial and subject sample sizes in neuroimaging. *NeuroImage*, *247*, 118786. https://doi.org/10.1016/j.neuroimage.2021.118786

Chen, Q., Wei, P., & Zhou, X. (2006). Distinct neural correlates for resolving stroop conflict at inhibited and noninhibited locations in inhibition of return. *Journal Of Cognitive Neuroscience*, *18*(11), 1937-1946. https://doi.org/10.1162/jocn.2006.18.11.1937

Chen, Q., Zhang, M., & Zhou, X. (2007). Interaction between location- and frequency-based inhibition of return in human auditory system. *Experimental Brain Research*, *176*(4), 630-640. https://doi.org/10.1007/s00221-006-0642-0

Chica, A. B., Bartolomeo, P., & Valero-Cabré, A. (2011). Dorsal and ventral parietal contributions to spatial orienting in the human brain. *The Journal of Neuroscience*, *31*, 8143 - 8149. https://doi.org/10.1523/JNEUROSCI.5463-10.2010

Chung, R. S., Cavaleri, J., Sundaram, S., Gilbert, Z. D., Del Campo-Vera, R. M., Leonor, A., Tang, A. M., Chen, K.-H., Sebastian, R., Shao, A., Kammen, A., Tabarsi, E., Gogia, A. S., Mason, X., Heck, C., Liu, C. Y., Kellis, S. S., & Lee, B. (2024). Understanding the human conflict processing network: A review of the literature on direct neural recordings during performance of a modified stroop task. *Neuroscience Research*, *206*, 1-19. https://doi.org/10.1016/j.neures.2024.03.006

Corbetta, M., & Shulman, G. L. (2002). Control of goal-directed and stimulus-driven attention in the brain. *Nature Reviews Neuroscience*, *3*(3), 201-215. https://doi.org/10.1038/nrn755

Cristescu, T. C., & Nobre, A. C. (2008). Differential modulation of word recognition by semantic and spatial orienting of attention. *Journal Of Cognitive Neuroscience*, *20*(5), 787-801. https://doi.org/10.1162/jocn.2008.20503

Danieli, K., Guyon, A., & Bethus, I. (2023). Episodic Memory formation: A review of complex Hippocampus input pathways. *Progress in Neuro-Psychopharmacology and Biological Psychiatry*, *126*, 110757. https://doi.org/10.1016/j.pnpbp.2023.110757

De Houwer, J. (2003). On the role of stimulus-response and stimulus-stimulus compatibility in the Stroop effect. *Memory & Cognition*, *31*(3), 353-359. https://doi.org/10.3758/bf03194393

Fox, M. D., Corbetta, M., Snyder, A. Z., Vincent, J. L., & Raichle, M. E. (2006). Spontaneous neuronal activity distinguishes human dorsal and ventral attention systems. *Proceedings of the National Academy of Sciences of the United States of America*, *103*(26), 10046-10051. https://doi.org/10.1073/pnas.0604187103

Friston, K. J., Zarahn, E., Josephs, O., Henson, R. N. A., & Dale, A. M. (1999). Stochastic designs in event-related fMRI. *NeuroImage*, *10*(5), 607-619. https://doi.org/10.1006/nimg.1999.0498

Fuentes, L. J., Boucart, M., Vivas, A. B., Alvarez, R., & Zimmerman, M. A. (2000). Inhibitory tagging in inhibition of return is affected in schizophrenia: evidence from the

stroop task. *Neuropsychology*, *14*(1), 134-140. https://doi.org/10.1037//0894-4105.14.1.134

Fuentes, L. J., Vivas, A. B., & Humphreys, G. W. (1999). Inhibitory tagging of stimulus properties in inhibition of return: Effects on semantic priming and flanker interference. *The Quarterly Journal of Experimental Psychology A: Human Experimental Psychology*, *52A*(1), 149-164. https://doi.org/10.1080/027249899391269

Funes, M. J., Lupiáñez, J., & Milliken, B. (2008). The modulation of exogenous Spatial Cueing on Spatial Stroop interference: Evidence of a set for "cue-target event segregation". *Psicológica*, *29*, 65-95.

Goebel, R., Esposito, F., & Formisano, E. (2006). Analysis of functional image analysis contest (FIAC) data with brainvoyager QX: From single-subject to cortically aligned group general linear model analysis and self-organizing group independent component analysis. *Human Brain Mapping*, *27*(5), 392-401. https://doi.org/10.1002/hbm.20249

Hanlon, F. M., Dodd, A. B., Ling, J. M., Bustillo, J. R., Abbott, C. C., & Mayer, A. R. (2017). From behavioral facilitation to Inhibition: The neuronal correlates of the orienting and reorienting of auditory attention. *Frontiers in Human Neuroscience 11*, 293. https://doi.org/10.3389/fnhum.2017.00293

Hayes, S. M., Nadel, L., & Ryan, L. (2007). The effect of scene context on episodic object recognition: parahippocampal cortex mediates memory encoding and retrieval success. *Hippocampus*, *17*(9), 873-889. https://doi.org/10.1002/hipo.20319

Holm, S. (1979). A Simple Sequentially Rejective Multiple Test Procedure. *Scandinavian Journal of Statistics*, *6*(2), 65-70. http://www.jstor.org/stable/4615733

Hu, F. K., Samuel, A. G., & Chan, A. S. (2011). Eliminating inhibition of return by changing salient nonspatial attributes in a complex environment. *The Journal of Experimental Psychology: General*, *140*(1), 35-50. https://doi.org/10.1037/a0021091

Kahneman, D., Treisman, A., & Gibbs, B. J. (1992). The reviewing of object files: Object-specific integration of information. *Cognitive Psychology*, *24*(2), 175-219. https://doi.org/10.1016/0010-0285(92)90007-o

Klein, R. M. (2000). Inhibition of return. *Trends Cogn Sci*, *4*(4), 138-147. https://doi.org/10.1016/s1364-6613(00)01452-2

Klein, R. M., & Dick, B. (2002). Temporal dynamics of reflexive attention shifts: a dual-stream rapid serial visual presentation exploration. *Psychol Sci*, *13*(2), 176-179. https://doi.org/10.1111/1467-9280.00432

Klein, R. M., & Ivanoff, J. (2011). The components of visual attention and the ubiquitous Simon effect. *Acta Psychologica*, *136*(2), 225-234. https://doi.org/10.1016/j.actpsy.2010.08.003

Klein, R. M., Redden, R. S., & Hilchey, M. D. (2023). Visual search and the inhibitions of return [Review]. *Frontiers in Cognition*, *Volume 2 - 2023*. https://doi.org/10.3389/fcogn.2023.1146511

Lepsien, J., & Pollmann, S. (2002). Covert reorienting and inhibition of return: an event-related fMRI study. *Journal Of Cognitive Neuroscience*, *14*(2), 127-144. https://doi.org/10.1162/089892902317236795

Li, A., Li, Y., He, X., & Zhang, Y. (2023). Inhibition of return as a foraging facilitator in visual search: Evidence from long-term training. *Attention, Perception, & Psychophysics*, *85*(1), 88-98. https://doi.org/10.3758/s13414-022-02605-0

Li, A., Miao, C., Han, Y., He, X., & Zhang, Y. (2018). Electrophysiological correlates of the effect of task difficulty on inhibition of return [Original Research]. *Frontiers in Psychology*, *9*. https://doi.org/10.3389/fpsyg.2018.02403

Li, M., Lu, S., & Zhong, N. (2016). The parahippocampal cortex mediates contextual associative memory: evidence from an fMRI study. *BioMed Research International*, *2016*, 9860604. https://doi.org/10.1155/2016/9860604

Li, Q., Yang, G., Li, Z., Qi, Y., Cole, M. W., & Liu, X. (2017). Conflict detection and resolution rely on a combination of common and distinct cognitive control networks. *Neuroscience & Biobehavioral Reviews*, *83*, 123-131. https://doi.org/10.1016/j.neubiorev.2017.09.032

Liu, J., Bayle, D. J., Spagna, A., Sitt, J. D., Bourgeois, A., Lehongre, K., Fernandez-Vidal, S., Adam, C., Lambrecq, V., Navarro, V., Seidel Malkinson, T., & Bartolomeo, P. (2023). Fronto-parietal networks shape human conscious report through attention gain and reorienting. *Communications Biology*, *6*(1), 730. https://doi.org/10.1038/s42003-023-05108-2

Liu, T. T. (2004). Efficiency, power, and entropy in event-related fMRI with multiple trial types: Part II: design of experiments. *NeuroImage*, *21*(1), 401-413. https://doi.org/10.1016/j.neuroimage.2003.09.031

Liu, T. T., & Frank, L. R. (2004). Efficiency, power, and entropy in event-related FMRI with multiple trial types. Part I: theory. *NeuroImage*, *21*(1), 387-400. https://doi.org/10.1016/j.neuroimage.2003.09.030

Liu, T. T., Frank, L. R., Wong, E. C., & Buxton, R. B. (2001). Detection power, estimation efficiency, and predictability in event-related fMRI. *NeuroImage*, *13*(4), 759-773. https://doi.org/10.1006/nimg.2000.0728

Luo, C., Lupiáñez, J., Fu, X., & Weng, X. (2010). Spatial Stroop and spatial orienting: the role of onset versus offset cues. *Psychological Research*, *74*(3), 277-290. https://doi.org/10.1007/s00426-009-0253-z

Lupiáñez, J. (2010). Inhibition of return. In A. C. Nobre & J. T. Coull (Eds.), *Attention and Time* (pp. 17–34). Oxford University Press. https://doi.org/10.1093/acprof:oso/9780199563456.003.0002

Lupiáñez, J., & Funes, M. J. (2005). Peripheral spatial cues modulate spatial congruency effects: Analysing the "locus" of the cueing modulation. *European Journal of Cognitive Psychology*, *17*, 727 - 752. https://doi.org/10.1080/09541440540000103

Lupianez, J., Klein, R. M., & Bartolomeo, P. (2006). Inhibition of return: Twenty years after. *Cognitive Neuropsychology*, *23*(7), 1003-1014. https://doi.org/10.1080/02643290600588095

Lupiáñez, J., & Milliken, B. (1999). Inhibition of return and the attentional set for integrating versus differentiating information. *Journal Of General Psychology*, *126*(4), 392-418. https://doi.org/10.1080/00221309909595373

Lupiáñez, J., Milliken, B., Solano, C., Weaver, B., & Tipper, S. P. (2001). On the strategic modulation of the time course of facilitation and inhibition of return. *Quarterly Journal Of Experimental Psychology*, *54*(3), 753-773. https://doi.org/10.1080/713755990

Lupiáñez, J., Ruz, M., Funes, M. J., & Milliken, B. (2007). The manifestation of attentional capture: Facilitation or IOR depending on task demands. *Psychological Research*, *71*(1), 77-91. https://doi.org/10.1007/s00426-005-0037-z

Ma, W. J., Navalpakkam, V., Beck, J. M., Berg, R., & Pouget, A. (2011). Behavior and neural basis of near-optimal visual search. *Nature Neuroscience*, *14*(6), 783-790. https://doi.org/10.1038/nn.2814

Martín-Arévalo, E., Chica, A. B., & Lupiáñez, J. (2014). Electrophysiological modulations of exogenous attention by intervening events. *Brain and Cognition*, *85*, 239-250. https://doi.org/10.1016/j.bandc.2013.12.012

Martín-Arévalo, E., Chica, A. B., & Lupiáñez, J. (2016). No single electrophysiological marker for facilitation and inhibition of return: A review. *Behavioural Brain Research*, *300*, 1-10. https://doi.org/10.1016/j.bbr.2015.11.030

Mayer, A. R., Dorflinger, J. M., Rao, S. M., & Seidenberg, M. (2004). Neural networks underlying endogenous and exogenous visual–spatial orienting. *NeuroImage*, *23*(2), 534-541. https://doi.org/10.1016/j.neuroimage.2004.06.027

Mayer, A. R., Franco, A. R., & Harrington, D. L. (2009). Neuronal modulation of auditory attention by informative and uninformative spatial cues. *Hum Brain Mapp*, *30*(5), 1652-1666. https://doi.org/10.1002/hbm.20631

Mayer, A. R., Harrington, D. L., Stephen, J., Adair, J. C., & Lee, R. R. (2007). An event-related fMRI Study of exogenous facilitation and inhibition of return in the auditory modality. *Journal Of Cognitive Neuroscience*, *19*(3), 455-467. https://doi.org/10.1162/jocn.2007.19.3.455

Mayer, A. R., Seidenberg, M., Dorflinger, J. M., & Rao, S. M. (2004). An event-related fMRI study of exogenous orienting: Supporting evidence for the cortical basis of inhibition of return? *Journal Of Cognitive Neuroscience*, *16*(7), 1262-1271. https://doi.org/10.1162/0898929041920531

Mayer, A. R., Teshiba, T. M., Franco, A. R., Ling, J., Shane, M. S., Stephen, J. M., & Jung, R. E. (2012). Modeling conflict and error in the medial frontal cortex. *Human Brain Mapping*, *33*(12), 2843-2855. https://doi.org/10.1002/hbm.21405

Menon, V., White, C. D., Eliez, S., Glover, G. H., & Reiss, A. L. (2000). Analysis of a distributed neural system involved in spatial information, novelty, and memory processing. *Hum Brain Mapp*, *11*(2), 117-129. https://doi.org/10.1002/1097-0193(200010)11:2<117::AID-HBM50>3.0.CO;2-M

Milham, M. P., Banich, M. T., Webb, A., Barad, V., Cohen, N. J., Wszalek, T., & Kramer, A. F. (2001). The relative involvement of anterior cingulate and prefrontal cortex in attentional control depends on nature of conflict. *Cognitive Brain Research*, *12*(3), 467-473. https://doi.org/10.1016/S0926-6410(01)00076-3

Milliken, B., Tipper, S. P., Houghton, G., & Lupiáñez, J. (2000). Attending, ignoring, and repetition: On the relation between negative priming and inhibition of return. *Perception & Psychophysics*, *62*(6), 1280-1296. https://doi.org/10.3758/BF03212130

Müller, N. G., & Kleinschmidt, A. (2007). Temporal dynamics of the attentional spotlight: Neuronal correlates of attentional capture and inhibition of return in early visual

cortex. *Journal Of Cognitive Neuroscience*, *19*(4), 587-593. https://doi.org/10.1162/jocn.2007.19.4.587

Nobre, A. C., & van Ede, F. (2018). Anticipated moments: Temporal structure in attention. *Nature Reviews Neuroscience*, *19*(1), 34-48. https://doi.org/10.1038/nrn.2017.141

Posner, M. I., & Cohen, Y. A. (1984). Components of visual orienting. *Attention and Performance*, *10*, 531-556.

Posner, M. I., Rafal, R. D., Choate, L. S., & Vaughan, J. (1985). Inhibition of return: Neural basis and function. *Cognitive Neuropsychology*, *2*(3), 211-228. https://doi.org/10.1080/02643298508252866

Prime, D. J., & Jolicoeur, P. (2009). On the relationship between occipital cortex activity and inhibition of return. *Psychophysiology*, *46*(6), 1278-1287. https://doi.org/10.1111/j.1469-8986.2009.00858.x

Ro, T., Farnè, A., & Chang, E. (2003). Inhibition of return and the human frontal eye fields. *Experimental Brain Research*, *150*(3), 290-296. https://doi.org/10.1007/s00221-003-1470-0

Satel, J., Wilson, N. R., & Klein, R. M. (2019). What neuroscientific studies tell us about inhibition of return. *Vision (Basel)*, *3*(4). https://doi.org/10.3390/vision3040058

Schmidt, C. C., Timpert, D. C., Arend, I., Vossel, S., Dovern, A., Saliger, J., Karbe, H., Fink, G. R., Henik, A., & Weiss, P. H. (2018). Preserved but Less Efficient Control of Response Interference After Unilateral Lesions of the Striatum. *Frontiers in Human Neuroscience*, *12*, 414. https://doi.org/10.3389/fnhum.2018.00414

Schmidt, C. C., Timpert, D. C., Arend, I., Vossel, S., Fink, G. R., Henik, A., & Weiss, P. H. (2020). Control of response interference: Caudate nucleus contributes to selective inhibition. *Scientific Reports*, *10*(1), 20977. https://doi.org/10.1038/s41598-020-77744-1

Seidel Malkinson, T., Bayle, D. J., Kaufmann, B. C., Liu, J., Bourgeois, A., Lehongre, K., Fernandez-Vidal, S., Navarro, V., Lambrecq, V., Adam, C., Margulies, D. S., Sitt, J. D., & Bartolomeo, P. (2024). Intracortical recordings reveal vision-to-action cortical gradients driving human exogenous attention. *Nature Communications*, *15*(1), 2586. https://doi.org/10.1038/s41467-024-46013-4

Taylor, T. L., & Donnelly, M. P. (2002). Inhibition of return for target discriminations: the effect of repeating discriminated and irrelevant stimulus dimensions. *Perception & Psychophysics 64*(2), 292-317. https://doi.org/10.3758/bf03195793

Taylor, T. L., & Klein, R. M. (1998). On the causes and effects of inhibition of return. *Psychonomic Bulletin & Review*, *5*(4), 625-643. https://doi.org/10.3758/BF03208839

Torres-Morales, C., & Cansino, S. (2024). Brain representations of space and time in episodic memory: A systematic review and meta-analysis. *Cognitive, Affective, & Behavioral Neuroscience*, *24*(1), 1-18. https://doi.org/10.3758/s13415-023-01140-1

Veen, V. V., & Carter, C. S. (2005). Separating semantic conflict and response conflict in the Stroop task: A functional MRI study. *NeuroImage*, *27*(3), 497-504. https://doi.org/10.1016/j.neuroimage.2005.04.042

Veen, V. V., Cohen, J. D., Botvinick, M. M., Stenger, V. A., & Carter, C. S. (2001). Anterior cingulate cortex, conflict monitoring, and levels of processing. *NeuroImage*, *14*, 1302-1308. https://doi.org/10.1006/nimg.2001.0923

Vivas, A. B., & Fuentes, L. J. (2001). Stroop interference is affected in inhibition of return. *Psychonomic Bulletin & Review*, *8*(2), 315-323. https://doi.org/10.3758/bf03196167

Vivas, A. B., Fuentes, L. J., Estevez, A. F., & Humphreys, G. W. (2007). Inhibitory tagging in inhibition of return: Evidence from flanker interference with multiple distractor features. *Psychonomic Bulletin & Review* *14*(2), 320-326. https://doi.org/10.3758/bf03194071

Vossel, S., Geng, J. J., & Fink, G. R. (2014). Dorsal and ventral attention systems: distinct neural circuits but collaborative roles. *Neuroscientist*, *20*(2), 150-159. https://doi.org/10.1177/1073858413494269

Wager, T. D., & Nichols, T. E. (2003). Optimization of experimental design in fMRI: a general framework using a genetic algorithm. *NeuroImage*, *18*(2), 293-309. https://doi.org/10.1016/S1053-8119(02)00046-0

Wang, Z., & Klein, R. M. (2010). Searching for inhibition of return in visual search: A review. *Vision Research*, *50*(2), 220-228. https://doi.org/10.1016/j.visres.2009.11.013

Weber, J. (2017). *NeuroElf (Version 1.1)*. In [Computer program]. http://neuroelf.net

Wilkinson, D., & Halligan, P. (2004). The relevance of behavioural measures for functional-imaging studies of cognition. *Nature Reviews Neuroscience*, *5*(1), 67-73. https://doi.org/10.1038/nrn1302

Wolfe, J. M., & Horowitz, T. S. (2017). Five factors that guide attention in visual search. *Nature Human Behaviour*, *1*(3), 0058. https://doi.org/10.1038/s41562-017-0058

Yang, Z., & Mayer, A. R. (2014). An event-related FMRI study of exogenous orienting across vision and audition. *Human Brain Mapping*, *35*(3), 964-974. https://doi.org/10.1002/hbm.22227

Zhang, M., & Zhang, Y. (2007). Semantic processing is affected in inhibition of return: evidence from an event-related potentials study. *Neuroreport*, *18*(3), 267-271. https://doi.org/10.1097/WNR.0b013e32801231a9

Zhang, Y., Zhou, X., & Zhang, M. (2012). Temporary inhibitory tagging at previously attended locations: evidence from event-related potentials. *Psychophysiology*, *49*(9), 1191-1199. https://doi.org/10.1111/j.1469-8986.2012.01412.x

Zhou, X., & Chen, Q. (2008). Neural correlates of spatial and non-spatial inhibition of return (IOR) in attentional orienting. *Neuropsychologia*, *46*(11), 2766-2775. https://doi.org/10.1016/j.neuropsychologia.2008.05.017

Zu, G., Zhang, T., Yang, J., Wang, A., & Zhang, M. (2023). Does the construction retrieval account apply to cross-modal inhibition of return in semantic context? *PsyCh Journal*, *12*(2), 211-221. https://doi.org/10.1002/pchj.618